

SUPPLEMENTARY INFORMATION

Unidirectional Self-actuation Transport of Liquid metal Nanodroplet in a Two-plate Confinement Microchannel

Erli Ni^a, Lin Song^b, Zhichao Li^a, Guixuan Lu^a, Yanyan Jiang^{a, c} and Hui Li^{a*}*

^a*Key Laboratory for Liquid-Solid Structural Evolution and Processing of Materials, Ministry of Education, Shandong University, Jinan 250061, China*

^b*State Key Laboratory of Solidification Processing, Northwestern Polytechnical University, Xi'an 710072, China*

^c*Shenzhen Research Institute of Shandong University, Shenzhen 518057, China.*

* Correspondence: yanyan.jiang@sdu.edu.cn (Y. J.); lihuilmy@hotmail.com (H. L.)

Table of contents

1. Adjust wettability by simply changing the characteristic energy parameter
2. The calculation details of the contact angle
3. The details of the scenario of being blocked by the contractive cross-section
4. why the effect of the oxide layer was not considered?
5. The details on the calculation of the interaction energy
6. The effect of the Concus-Finn criterion
7. Movie about the motion process under different channel parameters

1. Adjust wettability by simply changing the characteristic energy parameter

The Lennard-Jones potential is the earliest proposed two-body potential model. ε means the potential well depth, reflecting the strength of the interaction attraction between two atoms. The L-J potential has the advantage of being able to describe different systems by varying the depth of the potential well. Therefore, in this work, we could quantitatively adjust wettability by simply changing the ε . The specific principles are as follows:

Young's equation is a key way to calculate the contact angle. As shown in eq. S1, Young's equation is closely related to three tensions (γ_S surface energy, γ_L surface tension and γ_{LS} interfacial tension)

$$\cos\theta = \frac{\gamma_S - \gamma_L}{\gamma_{LS}} \quad (\text{S1})$$

According to the theory of Owens *et al.*¹, the surface tension or surface energy can be divided into the dispersion component γ^d and polar component γ^p . The dispersion component describes the non-polar interaction with van der Waals force.

$$\gamma = \gamma^d + \gamma^p \quad (\text{S2})$$

When the liquids come into contact with the solid substrates, interfacial tension will be generated. The effect of interfacial attraction on the tension in the interface can be predicted by the geometric mean of the dispersion force components of the surface tension of the liquids γ_L^d and of the solid γ_S^d . In this paper, the liquid metal droplet is not affected by the polar component, so the polar component could be ignored. Then, the tension in the interfacial region of the solid is equal to $\gamma_S - \sqrt{\gamma_S^d \gamma_L^d}$. Similarly, in the interfacial region of liquid, the attractive force of liquid is partially balanced by the attractive force of the solid and the tension in this layer is equal to $\gamma_L - \sqrt{\gamma_S^d \gamma_L^d}$. Since the interfacial tension γ_{LS} is the sum of the tensions in these two layers

$$\gamma_{LS} = \gamma_L + \gamma_S - 2\sqrt{\gamma_S^d \cdot \gamma_L^d} \quad (\text{S3})$$

Here, the correlation between the young's contact angle and the dispersion component can be obtained:

$$\cos\theta = -1 + 2\frac{\sqrt{\gamma_S^d \cdot \gamma_L^d}}{\gamma_L} \quad (\text{S4})$$

It can be seen that the contact angle is mainly related to the non-polar interaction with van der Waals force between the droplet and the solid substrate. The potential well depth ϵ of Lennard-Jones potential can felicitously represent this interaction potential. Therefore, we achieve different wettability of gallium droplets on the substrate by changing ϵ .

There are many studies using this method to control wettability in molecular dynamics (MD) simulations. For example, Bertrand *et al.*² have created a wetting gradient surface by controlling ϵ to model the dewetting of solid surfaces by partially wetting thin liquid films; Chakraborty *et al.*³ have simulated the droplet motion on a surface with chemical energy induced wettability gradient, where the different liquid-wall Lennard-Jones interaction parameters are used to achieve the chemical wettability gradient; Mahmood *et al.*⁴ have analyzed the unidirectional spontaneous transport of a water nanodroplet on a solid surface with a multi-gradient surface inspired by natural species. The energy parameter of the hydrophobic region is set as 1, 5, 10, 20, 30, and 40 meV to alter the intensity of the wettability gradient of the two surfaces.

2. The calculation details of the contact angle

Firstly, we introduce the cylindrical coordinate (r, z) for arbitrary point P, as **Figure S1 a, b**⁵. The z -axis is defined as the axis passing through the center of mass of the droplet and normal to x, y -plane. r is the distance from the z -axis. Then the simulation box is meshed into cylindrical bins with $\Delta r = 1 \text{ \AA}$, $\Delta z = 1 \text{ \AA}$. The density of each bin is calculated as the average over time of the bins. Then gathering densities of all the bins, and refining them using a linear interpolation algorithm, we can obtain the density profile and isochore profile of the droplet as shown in **Figure S1 d**. Subsequently, these interface points are adjusted by circular fit based on the least-squares method. The contact angle of the gallium droplet is obtained from the slope at the intersection with

the graphene sheet, show as **Figure S1 c**. Note that the interface points below a height of 0.02 are excluded, to avoid the influence of density fluctuations near the interface.

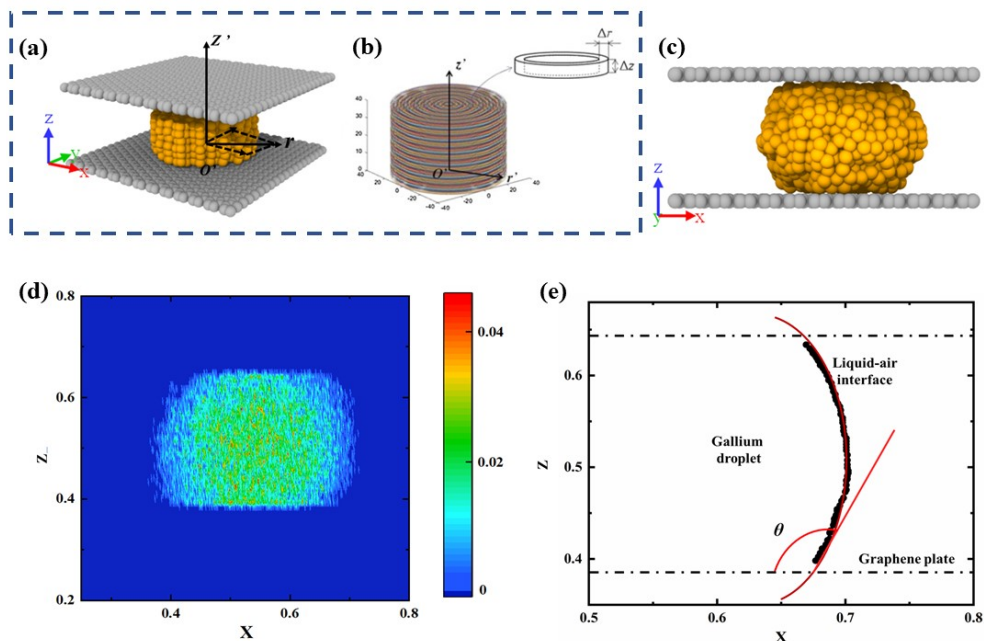


Figure S1 (a) Cylindrical coordinate system and (b) meshing. (c) (d) Density profile of gallium droplet. (e) The circular fit of the droplet interface.

3. The details of the scenario of being blocked by the contractive cross-section

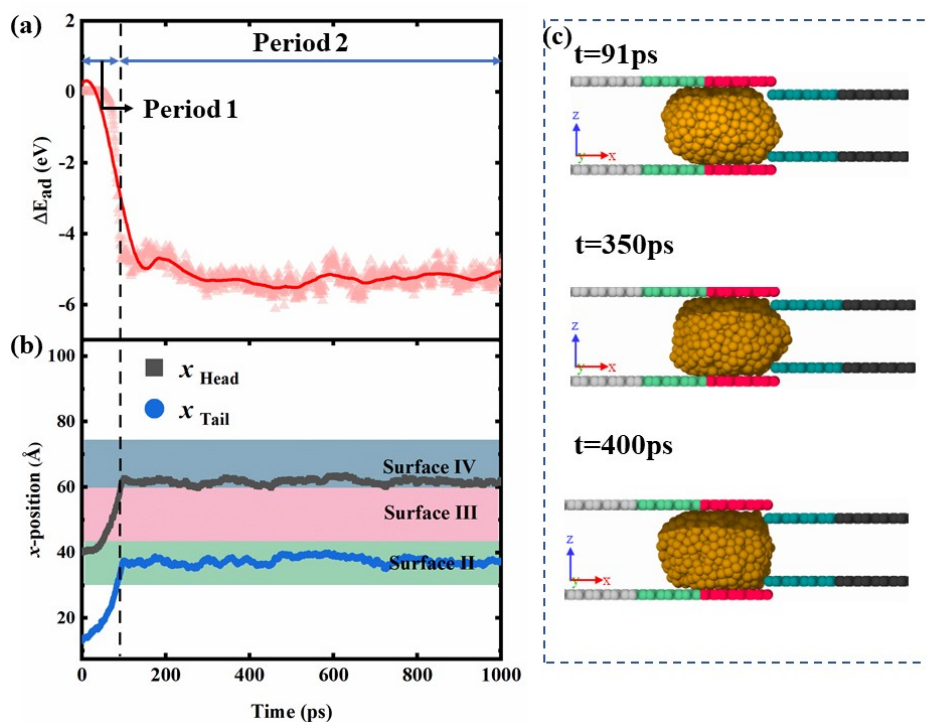


Figure S2 (a) Variation in ΔE_{ad} and (b) x-positions of the droplet's head and tail for passing through the contractive cross-section. ($\Delta\varepsilon=1.2 \times 10^{-3} eV$ and $\Delta H=6 \text{ \AA}$); (c) Snapshots of the positions of the gallium droplet in the contractive cross-section at different time points.

Figures S2 a and b show that the variation in ΔE_{ad} and the head and tail positions of the droplet over time for the case where the gallium nanodroplet is blocked by the contractive cross-section at $\Delta\varepsilon=1.2 \times 10^{-3} eV$ and $\Delta H=6 \text{ \AA}$. This case could be divided into two different periods. In the first period, droplet is accelerated and touches the leading edge of the contractive cross-section. In the second stage, the gallium nanodroplet briefly contacts Surface IV, but the droplet cannot enter the contractive cross-section at all. Then, the droplet exits to Surface III because ΔH is too large. Finally, the droplet would stay in front of the contractive cross-section as shown in **Figure S2 c**. Over the whole process, ΔE_{ad} is basically provided by $E_{ad,3}$.

4. Why the effect of oxide layer was not considered?

Gallium and its alloys react with oxygen to form a native oxide that encapsulates the liquid metal with a solid “skin”.⁶ This oxide layer is often considered a nuisance because it sticks to many surfaces-much like wet paint-which makes gallium difficult to use for fluidic applications. The oxide also provides a physical, chemical, and electrical barrier that prevents the metal from making direct contact with its surroundings. In addition, the oxide interferes with electrochemical measurements,

which makes gallium difficult to use for electro-chemistry. In addition, oxide “skin” would lead to enormous contact angle hysteresis and complicates the interpretation of contact angle measurements relative to conventional liquids such as water.⁷ Therefore, rheological characterization of the oxide skin is paramount for understanding and controlling liquid metals.⁸ However, in this paper, we did not consider the effect of oxide layer on the theoretical results. There are two main reasons.

On one hand, the simulated system does not contain oxygen and resembles a vacuum environment. Therefore, gallium droplets in our simulation will not be oxidized. Though MD simulation results cannot fully reflect the real phenomenon because the effect of scale effect and the lack of potential function, we could explore many properties from the microscopic view by analyzing the interaction potential and simulated phenomenon. Many studies have been conducted to explain the wetting or interfacial properties of gallium by molecular dynamics simulations^{9, 10}. In addition, there are many ways to prevent or delay gallium oxidation under experimental conditions, such as acidic environment¹¹ and vacuum environment. Such environmental conditions can be realized in microfluidic system¹².

On the other hand, this paper not only proposes a new approach to accelerate liquid metal nanodroplets by using wetting gradient, but also studies how the channel parameters affect the self-actuation of the nanodroplet. The proposed models are nearly insensitive to the kinds of liquids, but highly dependent on the wettability of a certain liquid droplet. That is, we can choose some other meaningful liquids to study. As is known, much work about the water self-actuation dynamics has been done and great

progress has been achieved in the experiment as the water is easily operated, while the liquid metal gets less attention because of requirement of complex experiment device and the oxide layer. However, the self-actuation dynamics of gallium-based droplets also plays a vital role in a wide variety of industrial processes and applications, such as microfluidics devices¹³, soft robots¹⁴, liquid sensors, as well as fluidic optical components¹⁵. which needs a better exploration. Therefore, considering the difficulty in experiment and the importance of its self-actuation dynamics, the gallium droplet is used and studied by performing MD simulations that can overcome the above drawbacks. More importantly, our results of the impact of the metallic droplets are expected to provide supplement and predict for the experimental study encountered in these applications related to the liquid metal.

5. The details on the calculation of the interaction energy

In this paper, A pairwise Lennard-Jones (LJ) potential was used to simulate the interaction between gallium atoms and carbon atoms. The interaction potential energy E_{Ga-C} is set in the process of simulation calculation, and we could output the interaction potential. It could reflect the interaction between groups very well.

The L-j potential is a mathematical model developed by Lennard-Jones in 1924 to describe the interaction between two neutral atoms or molecules. The L-J equation used in this paper is expressed as follows:

$$E_{LJ} = 4\varepsilon \left[\left(\frac{\sigma}{r} \right)^{12} - \left(\frac{\sigma}{r} \right)^6 \right], r < r_c \quad (S5)$$

Where σ is the distance parameter and the ε means characteristic energy parameter. r

is the distance between a pair of atoms. According to equation S5, we can deduce the force between a pair of atoms.

$$f = -\frac{\partial E_{LJ}}{\partial r} = 24 \frac{\epsilon r}{\sigma^2} \left[2 \left(\frac{\sigma}{r} \right)^{14} - \left(\frac{\sigma}{r} \right)^8 \right] \quad (\text{S6})$$

In Equation S5, $\left(\frac{\sigma}{r} \right)^{12}$ and $\left(\frac{\sigma}{r} \right)^6$ correspond to the repulsive and attractive terms. The repulsion term is mainly used to calculate the repulsion caused by the coincidence of electron orbits when the electron is far enough apart. The attraction term is mainly used to describe the attraction caused by the action of dipole moments (such as van der Waals forces and dispersion forces). When the distance between atoms is small, the repulsive term plays a dominant role and the two atoms repel each other. On the contrary, when the distance between atoms is large, the attraction term plays a dominant role and the two atoms are attracted to each other. As the distance between the atoms approaches infinity, the potential energy is zero and there is almost no interaction between the atoms. In practical calculation, to save time, the range of L-J action potential is usually set, namely the truncation radius. When the distance between atoms exceeds the truncation radius, the system considers the potential energy is zero.

The determination of L-J parameter is empirical and its rationality depends on the accuracy of experimental data. In addition, experimental data are always derived within a narrow temperature and pressure range, and when operating conditions deviate from this range, the L-J parameter may not be appropriate. For some new working fluids lacking experimental data, it is necessary to calculate the intermolecular equilibrium

distance based on first principles, and then infer a reasonable potential well depth value based on experimental data. In this paper, the selected distance parameter and characteristic energy parameter have been verified, which conform to the actual physical phenomenon.

L-J potential is not only simple in expression and less in resource consumption, but also can well describe the interaction between non-bonding atoms in the system. Therefore, it is widely used to simulate and predict the physical reactions caused by the solid-liquid interface interaction, such as wetting, anti-wetting and atomic rearrangement.

6. The effect of Concus-Finn criterion

Our work mainly focuses on the effect of the channel parameters on self-actuation in the contractive cross-sections microchannel. However, the Concus-Finn criterion rule pays more attention to the local dynamics of the liquid when the droplet passes through the obstacle. Therefore, to simplify the model, we apply the modified Lucas–Washburn equation globally to delineate the self-actuation behaviors of gallium nanodroplets. Furthermore, to ensure that obstacles cannot pin the contact lines in our system, we carefully study the effect of the Concus-Finn criterion on our work. The details are as follows:

A key problem with capillary filling in the presence of topological barriers (rectangular ridges) on the channel wall is that the contact line pins as a result of a geometric singularity in the meniscus stability make it difficult for the liquid to cross the topological barriers¹. The Concus-Finn criterion is proposed to solve this problem¹⁶. According to the Concus–Finn criterion, it is difficult for the liquid to cross the obstacle, provided the contact angle fulfills the following condition²:

$$\theta > \frac{\pi}{2} - \alpha \quad (0 < \theta < \frac{\pi}{2}) \quad (\text{S7})$$

$$\pi - \theta < \frac{\pi}{2} - \alpha \quad \left(\frac{\pi}{2} < \theta < \pi\right) \quad (\text{S8})$$

Here, θ is contact angle and the sides of obstacle make an angle of 2α with respect to the wall. In this study, gallium droplets present the unwetting state on the graphene

plates, that is, the contact angle is greater than $\frac{\pi}{2}$. Therefore, the condition that the

contact lines are pinned by obstacles in our system is $\theta < \frac{3\pi}{4}$. As shown in **Figure 1**,

the contact angle is generally less than $\frac{3\pi}{4}$, indicating that the self-actuation at the contractive cross-section is not limited by the Concus–Finn criterion.

In addition, the distance x traveled by the moving interface (The leading edge of the liquid–solid interface in the x -direction, as shown in **Figure S3 a**) in the microchannel over time has been studied. Because the Concus–Finn criterion is insensitive to obstacle size, we choose the contraction section with $\Delta H = 0.5 \text{ \AA}$ as the representative, which is conducive to better exclude the influence of step height, so as to judge whether the droplet movement is affected by the Concus–Finn criterion or not.

As shown in the **Figure S3 a**, in all cases, the front is slowed down right after meeting the obstacle. In close proximity to the steps, the front deforms in response to the geometrical discontinuity, climbs up the obstacle. Then, according to the Concus–Finn criterion, the front overcomes the obstacle and completely pass through the contractive cross-section. Manifestly, the Lucas–Washburn law is strongly violated in the vicinity of the obstacle. After overcoming the obstacle, the usual Lucas–Washburn regime is recovered, although after a transitional period of time, which depends on the wettability θ , and with a reduced velocity. Furthermore, by comparing our results with those of S. Chibbaro *et al.*¹⁷, the motion rule of gallium droplets completely conforms to the condition that the contact line is not pinned by obstacles (the case of $\theta=32, 40, 50$ in **Figure S3 b**).

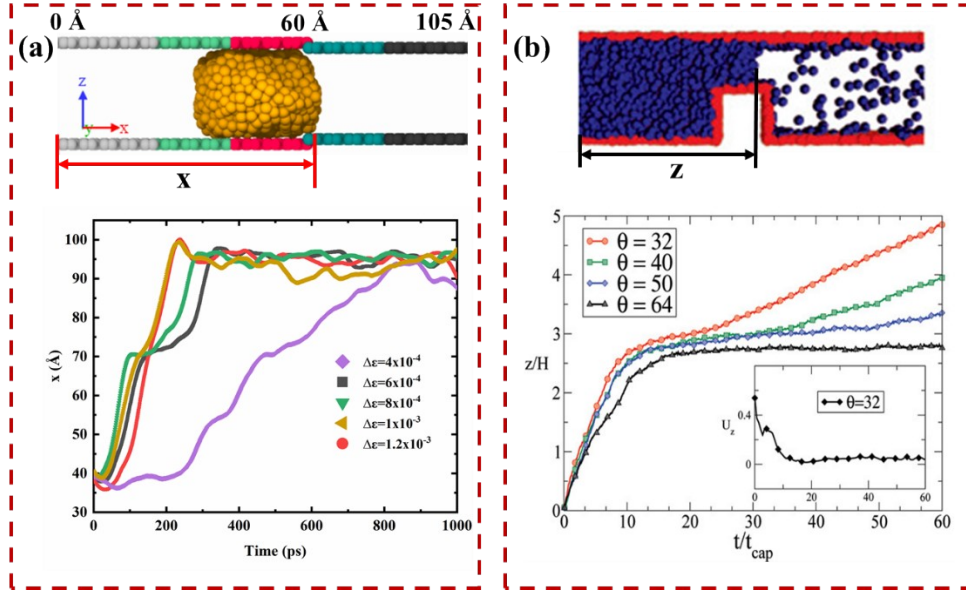


Figure S3 (a) The distance x traveled by the moving interface; (b) Time evolution of the interface midpoint while crossing the obstacle (S. Chibbaro et al.).

7. Supplementary Movies

Movie 1 The motion process of the liquid gallium nanodroplet in the two-plate confinement microchannel. The wetting gradient is set as $\Delta\varepsilon = 2 \times 10^{-4} eV$.

Movie 2 The motion process of the liquid gallium nanodroplet in the two-plate confinement microchannel. The wetting gradient is set as $\Delta\varepsilon = 6 \times 10^{-4} eV$.

Movie 3 The motion process of the liquid gallium nanodroplet in the two-plate confinement microchannel. The wetting gradient is set as $\Delta\varepsilon = 1 \times 10^{-3} eV$.

Movie 4 The motion process of the liquid gallium nanodroplet in the contractive cross-section microchannel. The channel parameters are set as $\Delta\varepsilon = 1.2 \times 10^{-3} eV$ and $\Delta H = 2 \text{ \AA}$. (The case of completely passing through the contractive cross-section)

Movie 5 The motion process of the liquid gallium nanodroplet in the contractive cross-section microchannel. The channel parameters are set as $\Delta\varepsilon = 1.2 \times 10^{-3} eV$ and $\Delta H = 4 \text{ \AA}$.

Å. (The case of partially passing through the contractive cross-section)

Movie 6 The motion process of the liquid gallium nanodroplet in the contractive cross-section microchannel. The channel parameters are set as $\Delta\varepsilon=1.2 \times 10^{-3} eV$ and $\Delta H=6$

Å. (The case of being blocked by the contractive cross-section)

References

1. F. M. Fowkes, *Industrial & Engineering Chemistry*, 1964, **56**, 40-52.
2. E. Bertrand, T. D. Blake, V. Ledauphin, G. Ogonowski, J. De Coninck, D. Fornasiero and J. Ralston, *Langmuir*, 2007, **23**, 3774-3785.
3. M. Chakraborty, A. Chowdhury, R. Bhusan and S. DasGupta, *Langmuir*, 2015, **31**, 11260-11268.
4. A. Mahmood, S. Chen, L. Chen, C. Chen, D. Liu, D. Weng and J. Wang, *Physical Chemistry Chemical Physics*, 2020, **22**, 4805-4814.
5. C. Huang, F. Xu and Y. Sun, *Computational Materials Science*, 2017, **139**, 216-224.
6. I. D. Joshipura, K. A. Persson, V. K. Truong, J.-H. Oh, M. Kong, M. H. Vong, C. Ni, M. Alsafatwi, D. P. Parekh, H. Zhao and M. D. Dickey, *Langmuir*, 2021, **37**, 10914-10923.
7. A. R. Jacob, D. P. Parekh, M. D. Dickey and L. C. Hsiao, *Langmuir*, 2019, **35**, 11774-11783.
8. M. D. Dickey, *ACS Applied Materials & Interfaces*, 2014, **6**, 18369-18379.

9. M. Yan, T. Li, P. Zheng, R. Wei and H. Li, *Physical Chemistry Chemical Physics*, 2020, **22**.
10. J. Wang, T. Li, Y. Li, Y. Duan, Y. Jiang, H. Arandiyan and H. Li, *Molecules*, 2018, **23**.
11. D. Kim, P. Thissen, G. Viner, D.-W. Lee, W. Choi, Y. J. Chabal and J.-B. Lee, *ACS Applied Materials & Interfaces*, 2013, **5**, 179-185.
12. N. Huang, M. Chen, S. Chen, K. Dang, H. Guo, X. Wang, S. Yan, J. Tian, Y. Liu and Q. Ye, *ACS Applied Materials & Interfaces*, 2021, **13**, 24487-24492.
13. K. Khoshmanesh, S.-Y. Tang, J. Y. Zhu, S. Schaefer, A. Mitchell, K. Kalantar-zadeh and M. D. Dickey, *LChip*, 2017, **17**, 974-993.
14. J. Wu, S.-Y. Tang, T. Fang, W. Li, X. Li and S. Zhang, *Advanced Materials*, 2018, **30**, 1805039.
15. J. Heikenfeld, P. Drzaic, J.-S. Yeo and T. Koch, *Journal of the Society for Information Display*, 2011, **19**, 129-156.
16. P. Concus and R. Finn, *Proceedings of the National Academy of Sciences*, 1969, **63**, 292.
17. S. Chibbaro, E. Costa, D. I. Dimitrov, F. Diotallevi, A. Milchev, D. Palmieri, G. Pontrelli and S. Succi, *Langmuir*, 2009, **25**, 12653-12660.